Carbohydrate Polymers 110 (2014) 320–328

Contents lists available at ScienceDirect

Carbohydrate Polymers

journal homepage: www.elsevier.com/locate/carbpol

Modified pullulan nanoparticles for oral delivery of lopinavir: Formulation and pharmacokinetic evaluation

Punna Rao Ravi*, Rahul Vats, Jagadeesh Balija, Sathya Prabhu Naidu Adapa, N. Aditya

Department of Pharmacy, BITS-Pilani Hyderabad Campus, Jawaharnagar, Ranga Reddy (Dist.), Andhra Pradesh, India

ARTICLE INFO

Article history:
Received 26 September 2013
Received in revised form 16 February 2014
Accepted 28 March 2014
Available online 13 April 2014

Keywords:
Pullulan acetate
Lopinavir
Nanoparticles
Physical characterization
Pharmacokinetic studies
Tissue distribution

ABSTRACT

In this investigation, we report the use of the pullulan acetate, a hydrophobic derivative of pullulan in the formulation of Lopinavir loaded nanoparticles meant for oral delivery. Pullulan was modified to pullulan acetate by acetylation process in the presence of pyridine; acetylation was confirmed by FT-IR and NMR spectra. Lopinavir, an HIV-protease inhibitor was formulated into nanoparticles of pullulan acetate by the well-known emulsion-solvent-evaporation method. The nanoparticles were tested for particle size, entrapment efficiency, in-vitro drug release and stability. Further, extensive pharmacokinetic and tissue distribution studies were performed in Wistar rats. The results showed that, with our method, we could obtain nanoparticles of ~197 nm, high entrapment efficiency (~75%) and monodisperse nature (PDI < 0.2). Stability data showed that the nanoparticles were stable over a period of 3 months. From the pharmacokinetic study data, we found that the relative bioavailability of Lopinavir from nanoparticles was ~2 folds higher than the free drug. Moreover, the tissue distribution study showed a higher distribution of Lopinavir loaded nanoparticles to lymphoid organs (liver, spleen and lymph nodes that are also important viral reservoirs in HIV infection). Thus, we conclude that Lopinavir loaded nanoparticle could be a superior alternative approach to free Lopinavir in treating HIV infection.

1. Introduction

Lopinavir (LPV) is a potent human immunodeficiency virus (HIV) protease inhibitor (PI) and an essential part of Highly Active Anti Retroviral therapy (HAART). It is used as a first line drug in HIV infected patients undergoing anti-retroviral therapy (Farmer et al., 2001). Being substrate of CYP3A4 and P-gp systems, LPV shows poor oral bioavailability in humans (du Plooy, Viljoen, & Rheeders, 2011; Ravi, Vats, Thakur, Srivani, & Aditya, 2012). Therefore, when given alone, like most of the other anti-retroviral drugs, LPV fails to achieve therapeutic concentration in blood and viral reservoirs (Chandwani1 & Shuter, 2008; Haase, 1999). The HIV mainly resides in anatomical (CNS, lymphatic system, liver, lungs and the genitals) and cellular reservoirs (*i.e.* CD+ T lymphocytes and monocytes/macrophages) of the human body (Schrager & D'Souza, 1998). Development of an effective drug delivery approach for the treatment of HIV/AIDS has been a global challenge (Levy, 2007, chap. 10).

Currently, the marketed formulation of LPV (Kaletra®, Abbott Laboratories) contains fixed dose combination of LPV and another PI, ritonavir. Ritonavir acts as a pharmacokinetic booster for LPV's bioavailability by inhibiting CYP3A4 and P-gp system (Zeldin & Petruschke, 2004). Although effective, RTV is known to cause glucose intolerance, gastrointestinal intolerance, lipid elevations, and perioral paresthesia (Shafran, Mashinter, & Roberts, 2005). Thus, there is a need for RTV-free strategy to improve LPV's oral bioavailability and also to achieve optimum LPV concentration in HIV localized sites in the body.

Nanoparticles (NPs) are considered to have wide applications for therapeutic purposes because of their distinctive characteristics (Sundar, Kundu, & Kundu, 2010). Due to their sub-cellular and submicron size, NPs can penetrate deep into the tissues through fine capillaries, cross the physiological barriers and are generally taken up efficiently by the reticulo-endothelial cells (Li & Huang, 2008).

Orally delivered NPs have shown significant improvement in cellular uptake and drug-plasma exposure (Ravi, Aditya, Kathuria, Malekar, & Vats, 2013; Ravi, Vats, Dalal, Gadekar, & Aditya, 2013). They accomplish this by avoiding first pass metabolism, P-gp mediated efflux or by promoting intestinal lymphatic transport (Kingsley et al., 2006). This allows for an efficient delivery of

* Corresponding author. Tel.: +91 40 66303539; fax: +91 40 66303998.
E-mail addresses: rpunnarao@hyderabad.bits-pilani.ac.in, rpunnarao@gmail.com (P.R. Ravi), rahulvats@hyderabad.bits-pilani.ac.in (R. Vats), jagadeesh20191@gmail.com (J. Balija), sathya.bitshyd@gmail.com (S.P.N. Adapa), aditya@hyderabad.bits-pilani.ac.in (N. Aditya).

http://dx.doi.org/10.1016/j.carbpol.2014.03.099
0144-8617/

therapeutic agents to target sites; the lymphoid organs and other HIV reservoirs of the human body (Trevaskis, Charman, & Porter, 2008).

Among the various NPs, biodegradable polymeric NPs have been widely explored as particulate carriers in pharmaceutical and medical fields (Hunter, Elsom, Wibroe, & Moghimi, 2012). Biodegradable, polymeric NPs provide an attractive alternative for long-term delivery of therapeutic agents meant for chronic administration (Feng, 2004). These drug loaded NPs cut overall cost of medicine, reduce risks of toxicity and are superior to conventional formulation. Control release, improved bioavailability, targeted delivery and improved therapeutic impact (Kumari, Yadav, & Yadav, 2010) are other advantages of NPs.

Pullulan is a non-toxic, non-immunogenic, biodegradable and neutral linear polysaccharide consisting of α-1,6 linked maltotriose residues. It is extensively used in food industry (Leathers, 2003). Pullulan cannot self-associate in aqueous solutions due to its high water solubility. Therefore, hydrophobized pullulan has been investigated as a drug delivery carrier to encapsulate lipophilic compounds (Akiyoshi, Deguchi, Moriguchi, Yamaguchi, & Sunamoto, 1993). Pullulan acetate (PA) is a well explored derivative of pullulan that can form self-aggregating mono-disperse NPs in aqueous media (Hong et al., 2011; Lee et al., 2012; Zhang et al., 2009).

This investigation deals with the synthesis and characterization of pullulan acetate (PA) polymer, its use in preparing LPV loaded pullulan acetate nanoparticles (PANPs). Further, characterization of PANPs such as particle size, morphology, drug encapsulation efficiency and *in vitro* drug release are reported. Comparative oral pharmacokinetic studies and tissue distribution studies of free LPV and LPV loaded PANPs were conducted in male Wistar rats to evaluate *in vivo* performance of prepared PANPs.

2. Experimental

2.1. Materials

LPV (purity > 99%) was obtained as a gift sample from Matrix Laboratories, Hyderabad, India. Pullulan (M_w = 200 kDa) was purchased from Hayashibara (Tokyo, Japan). Rat intestinal microsomes (RIM), rat liver microsomes (RLM) and NADPH were procured from BD Gentest, Woburn, USA. HPLC grade acetonitrile, ammonium acetate, heparin, methanol, methylene chloride (DCM), potassium dihydrogen phosphate and sodium citrate were purchased from Merck Laboratories, Mumbai, India. Methyl cellulose (molecular weight 14 kDa, viscosity 15 cps) and Tween 80 were purchased from S.D. Fine Chemicals Ltd, Mumbai, India. A Milli-Q water purification system (Millipore, MA, USA) was used for obtaining high quality HPLC grade water.

2.2. Methods

2.2.1. Synthesis of pullulan acetate

Pullulan acetate (PA), as hydrophobized pullulan, was synthesized by previously reported Motozato's method (Motozato, Ihara, Tomoda, & Hirayama, 1986). Briefly, 2 g of pullulan was dissolved by vigorous stirring in 20 ml of formamide maintained at 54 °C. For acetylation of pullulan, 6 ml pyridine and 15 ml of acetic anhydride was added to the above solution while maintaining the temperature at the 54 °C for 48 h. A dark-brown precipitate was obtained that was further purified by triturating with 1000 ml distilled water and 500 ml methanol. The solid material was vacuum-dried for 24 h, to finally obtain the product.

2.2.2. FT-IR spectroscopy

Fourier transform infrared (FTIR) spectra of pullulan and PA were recorded on a FT-IR 4200 (JASCO, USA) spectrometer in the range of 4000–400 cm^{-1} by KBr pellet method (1% sample in KBr). The samples were vacuum dried before FT-IR scan. Total of 40 scans were taken for each sample.

2.2.3. ^1H NMR spectroscopy

The proton nuclear magnetic resonance (^1H NMR) spectra were recorded on a Shielded Varian Inova spectrometer at 500 MHz (International Equipment Trading Ltd., Vernon Hills, USA) using tetramethylsilane (TMS) as an internal standard. Samples were dissolved in deuterated dimethyl sulfoxide (DMSO-d_6) before analysis. All NMR spectra were acquired at ambient temperature.

The degree of substitution (DS) in PA for acetyl groups was calculated from the integration value of acetyl protons (A) observed at 1.8–2.2 ppm and the OH protons and H-1 to H-6 protons (B) of pullulan moiety observed at more than 3.5 ppm. The DS values were calculated by the NMR method using following equation: DS = 10A/(3B + A), derived from the equation: $A/3x = B/\{7 + (3 - x)\}$ (corresponding to the area for one hydrogen in a glucose unit), where x equals DS [17].

2.2.4. Preparation of PANPs

LPV loaded PANPs were prepared according to the previously reported oil-in-water emulsion-solvent evaporation technique (Byun et al., 2011) with minor modifications. Briefly, accurately weighed quantities of LPV (10 mg) and PA (100 mg) were dissolved in 5 ml of DCM, this constituted organic phase. To form the primary emulsion, the organic phase was dropped into 50 ml aqueous PVA (0.5%, w/w) solution by means of a syringe fitted with needle (Internal diameter – 0.75 mm), positioned a few centimeters above the surface of the medium under gentle magnetic stirring (800 rpm). The primary emulsion was further subjected to high speed homogenization (at 5000 rpm, Polytron PT 3100D, Kinematica, Switzerland) for 15 min. The resulting colloidal preparation was centrifuged at 20,000 × g for 45 min to obtain LPV loaded PANPs. To remove the adherent free drug and excess PVA, the pellet was re-suspended in deionized water and centrifuged three times at 20,000 × g for 15 min each. Washed NPs were re-suspended in deionized water and subjected to pre-freezing at −80 °C for 6 h. Further, freeze-drying was carried for 24 h at −110 °C in a lyophilizer (Coolsafe 110-4, Scanvac, Denmark). Mannitol (5%, w/v) was used as a cryoprotectant. This lyophilized powder was stored in sealed glass containers at room temperature till further use.

2.2.5. Particle size analysis

Particle size, size distribution and zeta potential of the prepared PANP dispersions were measured by Zetasizer (Nano ZS, Malvern Instruments Ltd., Worcestershire, UK). All the samples were suitably diluted with double distilled water before measurement. Backscattering was measured by a detector at an angle of 173°. Instrument temperature was set at the 37 °C during the measurement. The result was described as mean ± S.D. (n = 6).

2.2.6. Scanning electron microscopy (SEM) analysis

PANPs were examined for morphology under scanning electron microscope (JSM-6360LV Scanning Microscope; Jeol, Tokyo, Japan). Before analysis, 100 μl of PANPs dispersion was dried overnight on an aluminum stub under vacuum. This was then sputter-coated with gold-palladium layer under an argon atmosphere using a gold sputter module in a high-vacuum evaporator (JFC-1100 fine coat ion sputter; Jeol, Tokyo, Japan). Coated samples were then scanned and photomicrographs were taken at an acceleration voltage of 15 kV.

2.2.7. Entrapment efficiency (EE) determination

Drug EE was determined by previously reported ultra-filtration method (Yue et al., 2009) with slight modification using microfilters (Amicon Ultra; MWCO; 10 kDa). Briefly, microfilters containing 0.5 ml of PANPs dispersion (suspended in water) were centrifuged at 6000 × *g* for 30 min to separate un-entrapped drug (free drug, W_{free}) from the total drug (W_{total}) added to the formulation. Un-entrapped drug (drug diffused through the membrane) was quantified by a previously validated RP-HPLC method (Vats, Murthy, & Ravi, 2011). EE and drug loading (DL%) were calculated by following equations:

$$EE\,(\%) = \left[\frac{(W_{\text{tota LPV}} - W_{\text{free LPV}})}{W_{\text{total LPV}}}\right] \times 100$$

$$DL\% = \left[\frac{(W_{\text{total LPV}} - W_{\text{free LPV}})}{(W_{\text{total LPV}} + W_{\text{total polymer}} - W_{\text{free LPV}})}\right] \times 100$$

where $W_{\text{total polymer}}$ is weight of pullulan acetate added to PANPs preparation.

Absence of membrane adsorption (non-specific binding) of LPV was confirmed by filtering LPV solution (1.5 μg/ml) prepared in phosphate buffer saline through microfilters. Recovery studies confirmed minimal adsorption of LPV (<1%).

2.2.8. In vitro release study

In vitro drug release study of PANPs was performed using the dialysis bag method (Shah & Pathak, 2010). Both free drug and LPV loaded PANPs were studied for *in vitro* release behavior. For the study, a sealed dialysis bag (MWCO, 12–14 kDa, pore size 2.4 nm), containing free drug or PANPs equivalent to 1.5 mg LPV was completely submerged in 50 ml drug release media (PBS containing 0.1%, w/v Tween 80, pH 7.4). The temperature of the media was maintained at 37 ± 0.5 °C and media was stirred at 50 rpm using magnetic bead. The drug release media were completely replaced at pre-determined time intervals to the maintain sink conditions. Cumulative release of LPV in sample solution was determined by previously RP-HPLC method (Vats et al., 2011).

Obtained data were fitted into zero order, first order, Higuchi and reciprocal-powered time mathematical models for evaluation of release kinetics. Regression coefficient (r^2) and time for 50% dissolution (t_{50}%) were calculated for the best-fit model.

2.2.9. Stability studies

Stability of prepared formulations was assessed as per International Conference on Harmonization (ICH) Q1A (R2) guidelines (ICH, 2003). Briefly, LPV loaded PANP suspensions were stored in sealed glass vials at 25 ± 2 °C/60 ± 5% RH in a stability chamber (Remi, Mumbai, India). Samples were analyzed over a three-month period for particle size, zeta potential, poly-dispersity index (PDI) and EE. Statistical evaluation was done using GraphPad Prism version 5.03 for Windows software (GraphPad Software, San Diego, USA).

2.2.10. In vitro metabolic stability study

In vitro metabolic stability studies were performed by incubating free LPV, free LPV with blank PANPs and LPV loaded PANPs with RIM and RLM (1 mg/ml) at an effective concentration of 5 μM. The reaction was initiated by addition of NADPH (2 mM) in phosphate buffer (100 mM, pH 7.4). Incubations were performed at 37 °C in a shaking water bath for 30 min. The reaction was terminated by addition of cold acetonitrile. Samples were vortexed briefly and centrifuged at 6,000 × *g* for 15 min. The resulting clean supernatant (75 μl) was injected into the HPLC. Percentage metabolism of LPV was determined in all the three test conditions. In a separate set of experiment, free LPV was incubated with reaction buffer without enzymes for 30 min to ensure stability of free LPV in the reaction buffer. No non-enzymatic degradation of LPV was observed (data not shown).

Enzyme inhibition due to formulation excipients present in PANPs was investigated by incubating blank NPs (NPs prepared without drug) along with free LPV; difference in metabolism (compared with free LPV alone) was taken as a sign of enzyme inhibition.

2.2.11. Oral pharmacokinetic evaluation of PANPs

Male Wistar rats, weighing 180–220 g, were used in this study. Experimental protocol was approved by the Institutional Animal Ethics Committee (Approval No.: IAEC-01/01-12). All the animals were housed under constant environmental conditions (22 ± 1 °C room temperature; 55 ± 10% relative humidity; 12 h light/dark cycle) and were allowed access to food and water *ad libitum*. Animals were fasted overnight (12 h) before dosing and continued on fasting until 4 h post administration of the formulation. Thereafter, rat chow diet was provided *ad libitum*. In all the studies, freshly prepared drug formulations were administered.

Pharmacokinetic studies were conducted following oral (20 mg/kg, 10 ml/kg) administration of free LPV suspension and LPV loaded PANPs. In pharmacokinetic studies, animals were randomly divided into two groups; group A (control) and group B (treatment) with five animals in each group. While the control group received free drug suspension (LPV suspended in 0.5%, w/v methyl cellulose), the treatment group received LPV loaded PANP formulation.

Blood samples (200 μl) were collected from the orbital sinus into microcentrifuge tubes containing anti-coagulant (3.8%, w/v sodium citrate) at pre-dose, 0.25, 0.5, 0.75, 1, 2, 3, 4, 6, 8 and 12 h post dose. These samples were kept on ice until further processing. Plasma was harvested from these by centrifuging at 4 °C for 10 min at 950 × *g*. The obtained plasma samples were stored at −70 °C until further analysis. Previously reported RP-HPLC method (Vats et al., 2011) from our lab was used to estimate LPV in rat plasma matrix.

2.2.12. Bio-distribution study of PANPs

Bio-distribution study of LPV was performed using 24 male Wistar rats (180 ± 20 g). Animals were randomly divided into two groups with 12 rats in each group. The animals were administered either free LPV suspension or LPV loaded PANPs at a dose of 20 mg/kg via oral gavage. Three rats from each group were sacrificed at 1st h and 4th h post dosing. Tissue samples were collected after perfusion with heparinized (5 international unit) saline (0.9%, w/v NaCl) through the hepatic portal vein. Perfusion was done to remove residual blood from the organs. Tissues of interest (liver, spleen and mesenteric lymph nodes) were collected and stored at −70 °C until further analysis.

Prior to analysis, tissue samples were thawed to room temperature, minced and homogenized to a fine paste (25%, w/v) in a tissue homogenizer (Remi, Mumbai, India) along with methanol:water (1:4) mixture. LPV was extracted from tissue homogenate by adding a protein precipitating agent, acetonitrile in the ratio 1:3 (v/v).

2.2.13. HPLC analysis

For analysis of rat plasma samples a validated RP-HPLC method (Vats et al., 2011) was used. In brief, the liquid chromatography system employed was Shimadzu HPLC (Shimadzu, Japan) with solvent delivery system of two pumps (Model LC-20AD, Prominence Liquid Chromatograph, Shimadzu, Japan), an auto injector (Model SIL-20A HT, Prominence Auto Sampler, Shimadzu, Japan) and photo diode array (PDA) UV detector (Model SPD-M20A, Prominence Diode Array Detector, Shimadzu, Japan). Chromatographic separation was achieved on a Phenomenex Luna® C18 (250 mm × 4.6 mm, 5 μm) column. To analyze LPV, an isocratic mobile phase consisting of a mixture of acetonitrile-ammonium acetate buffer (10 mM, pH 6.5)

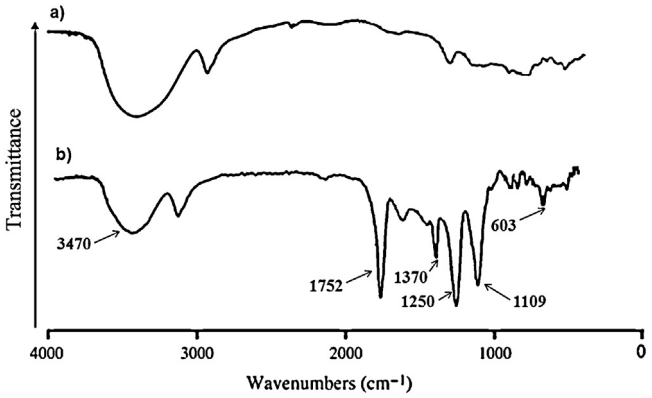

Fig. 1. FT-IR spectra of pullulan (a) and pullulan acetate (b).

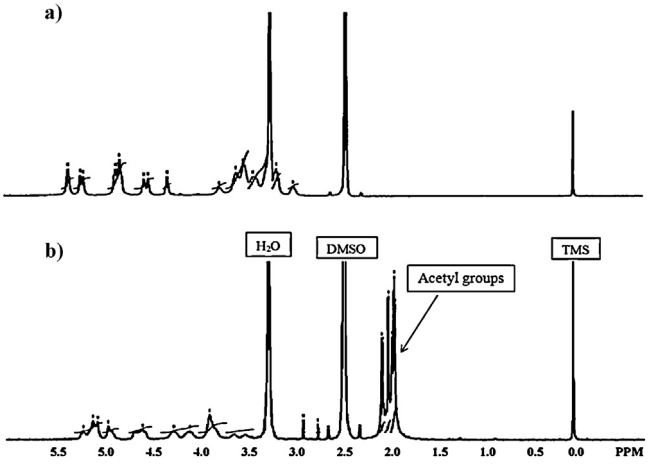

Fig. 2. ^{1}H NMR spectra of pullulan (a) and pullulan acetate (b) in DMSO-d_6.

(65:35, v/v) was delivered at a flow rate of 1.0 ml/min into the HPLC system. LPV was monitored at a wavelength of 210 nm.

The above reported method was partially validated for the analysis of drug in mesenteric lymph node, spleen and liver tissue matrices. No interference was observed by tissue matrices at the retention time of LPV. The method was found to be reproducible with a good recovery (>90%) for the drug.

A single step protein precipitation technique was followed for extraction of LPV from the rat plasma matrix and tissue samples. In 100 μl of drug spiked samples, 300 μl acetonitrile was added and vortex mixed for 2 min. Extracted samples were centrifuged (8000 × *g* for 15 min) and resultant clean supernatant (75 μl) was injected into the HPLC to determine the concentration of the drug in the samples.

The detector response was linear over the concentration range of 200 ng/ml to 4000 ng/ml. Lowest limit of quantification was found to be 200 ng/ml in all the biological matrices (plasma and tissues).

2.2.14. Statistical analysis

All *in vitro* studies were performed in triplicate and data from these experiments are expressed as mean ± SD. Non-compartmental pharmacokinetic analysis was performed using Phoenix® WinNonlin® (Pharsight Inc., Mountain view, CA, USA) to determine various pharmacokinetic parameters. Unpaired *t-test* or Analysis of Variance (ANOVA), followed by Dunnett's test (Graphpad Prism, version 5.03) was used to assess any significant difference between means. The significance level was set at 5%.

3. Results and discussion

3.1. Synthesis and characteristics of PA

PA was synthesized by replacing free hydroxyl groups present in glucose units of pullulan with the acetate groups. Comparison of the FT-IR spectra of pullulan (Fig. 1(a)) and PA (Fig. 1(b)) confirms the introduction of acetate groups in PA (Fig. 1(b)), as indicated by the C=O stretching at 1752 cm^{-1}, C–O stretching at 1250 cm^{-1} and 1109 cm^{-1}, CH_3 deformation at 1370 cm^{-1} and presence of O–C=O bend at 603 cm^{-1}. The peak at 3470 cm^{-1} originating from stretching vibration of the hydroxyl (–OH) group became relatively weak following acetylation in PA further indicating the substitution of free –OH groups.

Comparative ^{1}H NMR spectra of pullulan and PA dissolved in DMSO-d_6 is shown in Fig. 2. Intensity of hydroxyl proton signals of PA observed at 4.5–5.6 ppm decreased in comparison with pullulan. The ^{1}H NMR spectra of PA also demonstrated the introduction of additional methyl proton signals at 1.8–2.2 ppm, which can be assigned to the acetyl groups. The acetylation of pullulan was successful with the procedure followed. However, we could not precisely assign few proton signals observed at 3 ppm and above due to the complexity of the signals.

The calculated value of DS, post acetylation, was 2.91. Results indicate that nearly all the hydroxyl (–OH) groups have been substituted by acetyl moiety. Higher DS would render more hydrophobicity to PA that could further accommodate more amount of drug thereby increasing the EE.

3.2. Physicochemical characterization of PANPs

The near sphericity of LPV loaded PANPs was evident from SEM photomicrograph (Fig. 3). Data from the particle size analysis demonstrated a unimodal size distribution of PANPs (profile is not shown). Mean particle size and the PDI of LPV loaded PANPs ($n = 6$) were 197 ± 4 nm and 0.11 ± 0.01 respectively. The low value of PDI indicates the usefulness of the proposed method in producing stable LPV PANPs with a relatively narrow size distribution. The mean zeta potential value of LPV loaded PANPs was −3 ± 1 mV. The negative zeta potential was attributed to the presence of ionized acetate residues on the polymeric matrix surface. The oil-in-water emulsion-solvent evaporation technique for NP preparation is widely reported method for encapsulation of hydrophobic compounds (Pinto, Neufeld, Ribeiro, & Veiga, 2006). The EE and DL studies demonstrated efficiency of the PANPs in entrapping LPV (EE, 76.5 ± 3.5%; DL, 6.9 ± 1.5%). High EE could be possibly due to hydrophobic interactions between LPV and modified polymer molecules.

3.3. In vitro drug release

In vitro drug release profile obtained from free LPV showed complete drug dissolution into the media within 5 h. On the contrary, LPV loaded PANPs showed bi-phasic release pattern, that was characterized by an initial rapid release (53%) in the first 8 h followed by a slow and continuous drug release up to 75 h (profile is not shown). The initial rapid release could be possibly due to the presence of LPV molecules on the surface of NPs (entrapped within a surfactant layer). In the second phase, slower release is seemingly due to slow diffusion of the entrapped drug from the matrix of NPs. Drug release kinetics were studied by fitting data into various mathematical models. From regression analysis, drug release from NPs was most appropriately described by reciprocal-powered time model ($r^2 = 0.988$). In comparison, zero-order kinetics ($r^2 = 0.287$), first-order kinetics ($r^2 = 0.939$) and Higuchi kinetics ($r^2 = 0.898$) showed relatively lower r^2 values. Times taken for 50% drug release ($t_{50\%}$)

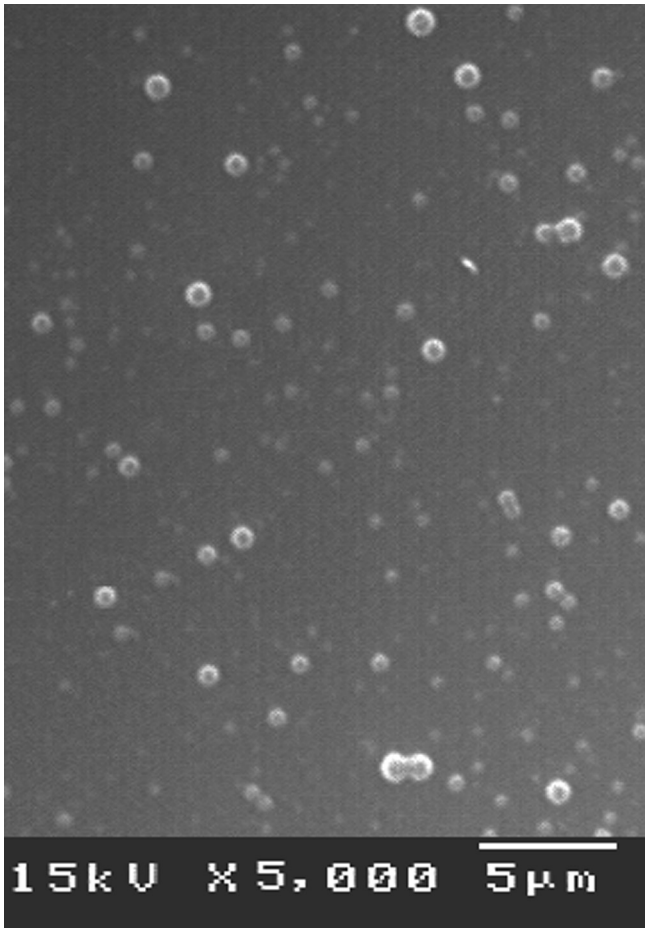

Fig. 3. Scanning electron microscopic image of LPV loaded PANPs.

and mean dissolution time (MDT) from NPs were calculated to be 6.96 h and 40.71 h respectively.

The drug release kinetics of encapsulated drugs in nanoparticles is a major determinant for its biological effect. Thus, evaluation of drug release kinetics is of paramount importance in the nanodrug delivery system. Mathematical modeling of drug release kinetics provides a basis for the study of mass transport mechanisms that are involved in the control of drug release (Yao & Weiyuan, 2010).

Reciprocal time release model takes into account both diffusion and dissolution controlled process. This model has been shown to be superior to other mathematical models for drug release from NPs (Mohammad et al., 2008). Moreover, the reciprocal time release model can also be used to get $t_{50\%}$ value. The bi-phasic drug release pattern from NPs can be useful in giving an initial loading dose (of loosely bound drug); later, drugs inside NPs can provide can provide a controlled release effect. This helps in improving mean retention time of the drug and its plasma exposure. Hence, the bioavailability of the drug improves s consequence of metabolic protection, lower clearance and increased retention (Gajendiran, Gopi, Elangovan, Murali, & Balasubramanian, 2013). Increased bioavailability also increases the therapeutic efficacy and reduces the overall dose of the drug.

3.4. Stability studies

Formulation stability of PANPs was evaluated by measuring particle size, zeta potential, PDI and EE at 0, 1, 2 and 3 months of storage at ambient temperature. As shown in Fig. 4, mean particle diameter and zeta potential of NPs were not significantly affected by storage at ambient temperature. From the same figure, small change in PDI values was observed over time. However, for all samples, upon storage, PDI values remained below 0.2 suggesting that the particle population remained fairly homogeneous without any significant aggregation in NP dispersion during storage. The particle stability of PANPs was attributed to steric stabilization effect of PVA. It is reported that PVA adsorbs onto the NP surface and creates a repulsive barrier that prevents particle aggregation (Lee, Tsai, & Yates, 2010). Furthermore, no appreciable change in EE was observed. In summary, from all the stability data, it can be concluded that the formulated PANPs were stable for at least 3 months upon storage at ambient temperature. However, extensive stability studies need to be performed to fix the shelf-life of PANPs in different storage conditions.

Table 1
Pharmacokinetic parameters of LPV following oral administration of free LPV and LPV PANPs to Wistar rats ($n = 5$).

Route	Parameters	Free LPV (Group A)	LPV PANPs (Group B)
Oral (LPV, 20 mg/kg)	C_{max} (ng/ml)	646.15 ± 67.70	1060.34 ± 86.51*
	T_{max} (h)	0.75 (0.5–1.0)	0.75 (0.5–1.0)
	MRT(h)	5.19 ± 0.19	6.75 ± 0.25*
	AUC (ng/ml h)	1739.52 ± 58.34	3782.50 ± 76.87**
	F_{rel}		2.2 ± 0.2

Statistically significant difference (*$p < 0.05$; **$p < 0.01$) as compared to Free LPV (Group A). The data are expressed as mean ± S.D. T_{max} values are expressed in range. LPV, lopinavir; PANPs, pullulan acetate nanoparticles; C_{max}, maximum plasma concentration; T_{max}, time to reach the maximum plasma concentration; MRT mean residence time; AUC, area under the curve; F_{rel}, relative bioavailability.

3.5. In vitro metabolic stability study of LPV

Results obtained from *in vitro* metabolic stability studies using RIMs and RLMs are shown in Fig. 5. Mean percentage metabolism of LPV in loaded PANPs (35% in RIMs; 29% in RLMs) was found to reduce significantly ($p < 0.001$) as compared to free LPV (90% in RIMs; 85% in RLMs). However, statistically no significant change in metabolism of free LPV was observed upon co-incubation with blank PANPs. This indicates that the excipients used in the manufacture of NPs did not inhibit CYP enzymes and an appreciable increase in bioavailability was due to inaccessibility of enzymes to degrade LPV entrapped in NPs.

3.6. Pharmacokinetic evaluation of PANPs

The *in vivo* behavior of PANPs was assessed by performing pharmacokinetic studies in male Wistar rats. Pharmacokinetic behavior of free LPV and PANPs in male Wistar rats after oral administration is shown in Fig. 6. Comparative pharmacokinetic parameters of free LPV and LPV PANPs are given in Table 1.

Following oral administration, LPV loaded PANPs showed statistically significant improvement in the pharmacokinetics of LPV as determined by AUC (increased by 2.2 folds, $p < 0.01$), C_{max} (increased by 1.7 folds, $p < 0.05$), and MRT (increased by 1.3 folds, $p < 0.05$). However, statistically no significant difference in T_{max} was observed as compared to free LPV.

From oral pharmacokinetic studies of free LPV, it is evident that LPV has poor bioavailability, presumably due to both high first-pass metabolism and P-gp efflux. Significant improvement in plasma exposure of LPV in PANPs could be attributed to reduced metabolism and/or P-gp efflux upon loading. A significant increase in LPV's MRT in plasma possibly indicates the metabolic protection (in the liver) by PANPs to LPV. Our results from *in vitro* metabolism studies agree with the *in vivo* pharmacokinetic data. However, we

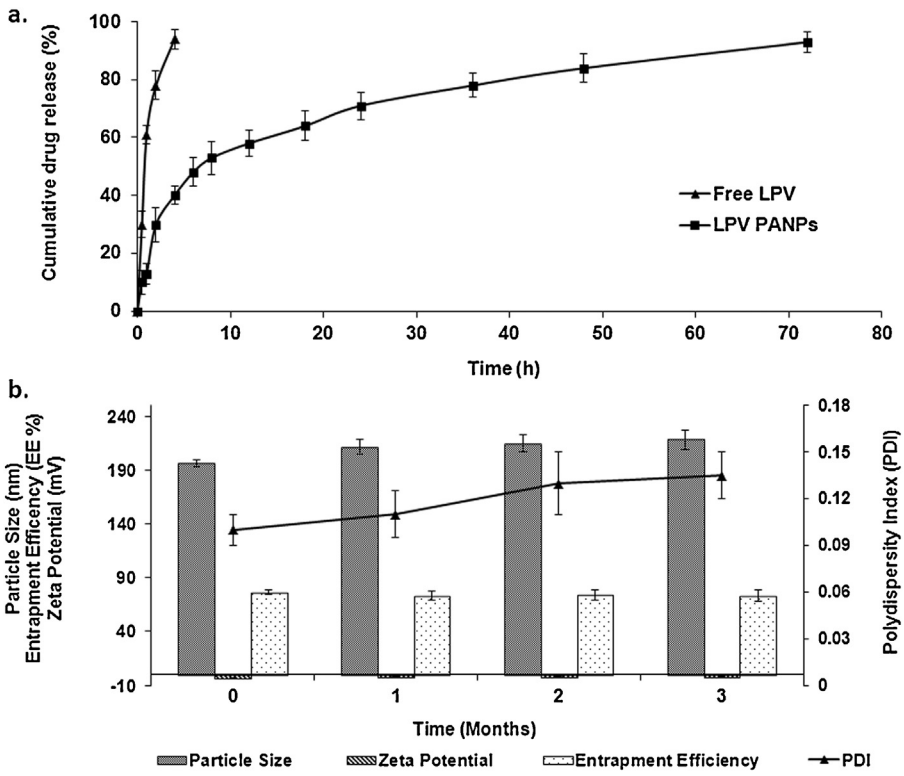

Fig. 4. (a) In-vitro drug release profile of free LPV and LPV loaded PANPs in phosphate buffer saline (PBS), pH 7.4 with 0.1% Tween 80. The data are expressed as mean ± S.D. of six independent determinations ($n = 6$). (b) The stability characteristics of LPV loaded PANPs in terms of mean particle size, polydispersity index (PDI) and entrapment efficiency (EE), stored at 25 ± 2 °C and 60% ± 5% RH. The data are expressed as mean ± S.D. of six independent determinations ($n = 6$). LPV, lopinavir; PANPs, pullulan acetate nanoparticles.

could not evaluate the possible role of P-gp in the pharmacokinetic modulation of PANPs.

In order to establish *in vivo* performance of LPV loaded PANPs at targeted organs, tissue distribution study was conducted and compared with the distribution pattern of free LPV. As shown in Fig. 7, LPV in loaded PANPs significantly accumulated in the liver, spleen and lymph node tissues in comparison to free LPV. Higher localization of LPV in liver tissue than other tissues could be possibly due to superior blood perfusion to the liver. The tissue distribution data are presented as an amount ratio of LPV. The amount ratio is a ratio of LPV from PANPs to free LPV. A higher value for this ratio indicates a lower rate of LPV clearance (*i.e.* accumulation) from the respective tissue; lower value indicates the opposite.

From Fig. 7, the amount ratio of LPV at 1st h in liver, spleen and lymph nodes were 1.5, 1.9 and 1.3 respectively. However, after 4 h of dosing, the values were found to be 2.5, 3.8 and 2.4 respectively.

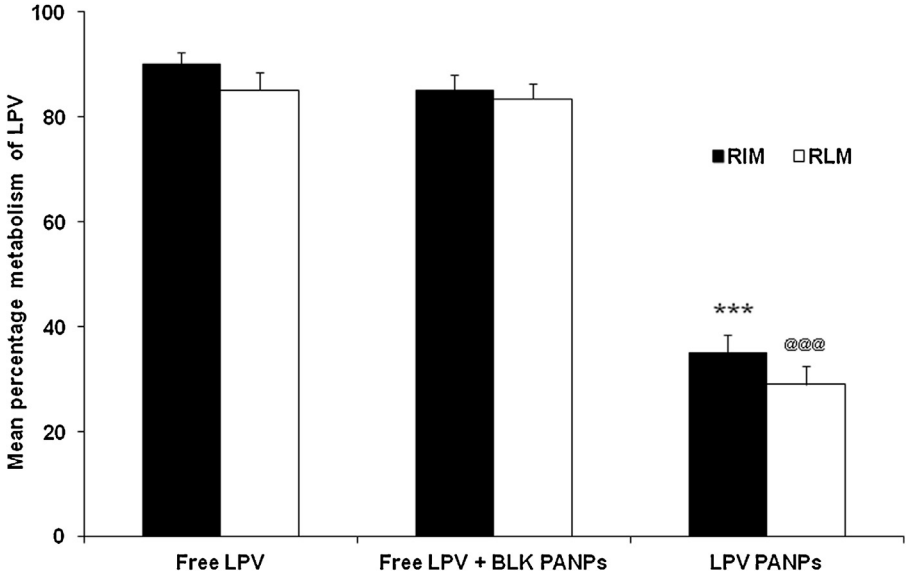

Fig. 5. Metabolic stability of free LPV and LPV loaded PANPs after 30 min incubation with RIM and RLM at 1 mg/ml protein concentration. ***Statistically significant difference ($p < 0.001$) as compared to Free LPV. The data are expressed as mean ± S.D. LPV, lopinavir; PANPs, pullulan acetate nanoparticles; RIM, rat intestinal microsomes; RLM, rat liver microsomes.

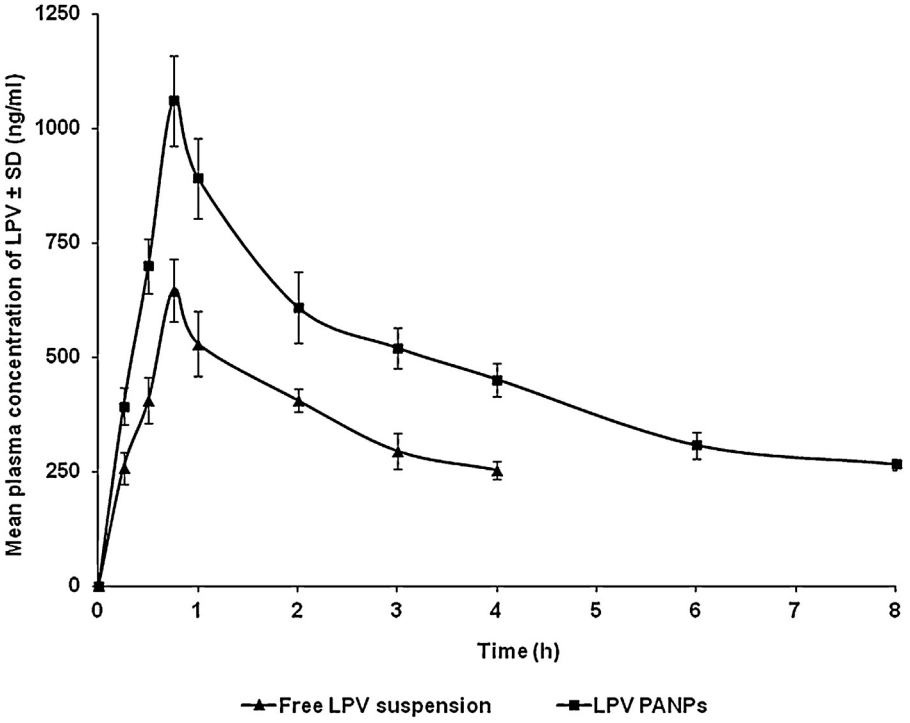

Fig. 6. Mean plasma concentration-time profile of LPV following oral administration (20 mg/kg) of free LPV and LPV loaded PANPs to Wistar rats ($n = 5$). The data are expressed as mean ± SD. LPV, lopinavir; PANPs, pullulan acetate nanoparticles.

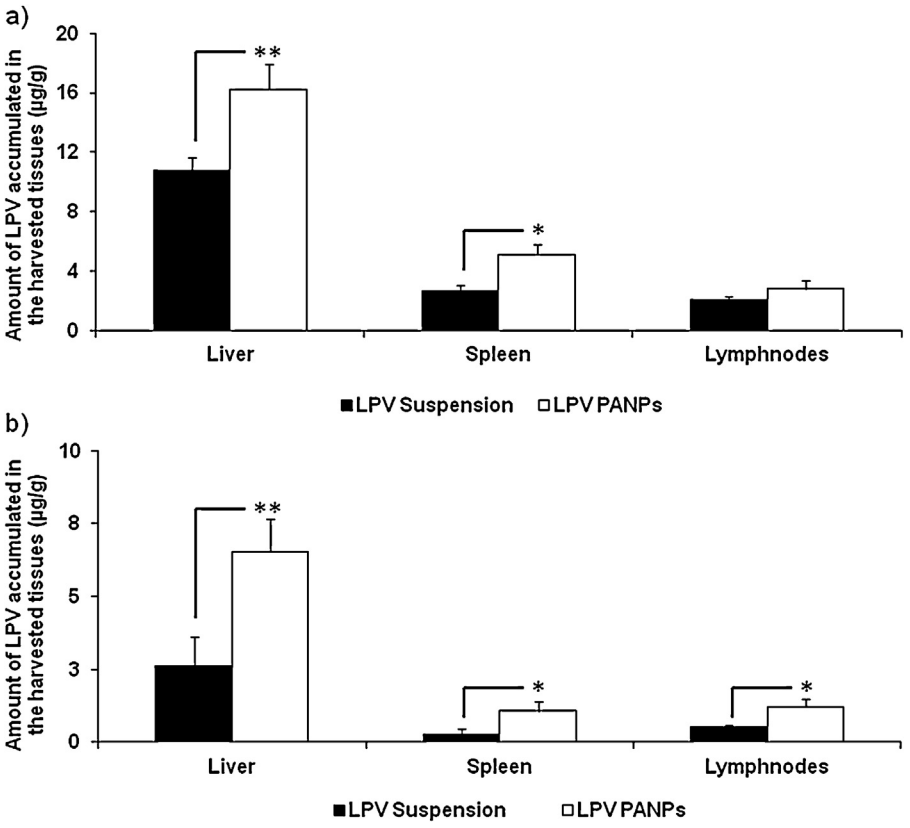

Fig. 7. Tissue distribution study of free LPV and LPV loaded PANPs following oral administration (20 mg/kg) to Wistar rats. Three animals were sacrificed at 1st h (a) and 4th h (b) post dosing to harvest liver, spleen and mesenteric lymph node tissues. Statistically significant difference (*$p < 0.05$; **$p < 0.01$) as compared to Free LPV. The data are expressed as mean ± S.D. LPV, lopinavir; PANPs, pullulan acetate nanoparticles.

Increasing value of amount ratio with time apparently indicates greater accumulation and hence lower clearance of LPV from PANPs than free LPV.

Further, selective accumulation of LPV PANPs in lymphoid organs is due to lymphatic uptake of NPs following oral administration. It has been reported that the M-cells covering Peyer's patches take up NPs by a combination of endocytosis and/or transcytosis mechanism (Albanese, Tang, & Chan, 2012). The size of these particles takes them to the lymphatic system through relatively larger openings rather than blood capillaries whose pore sizes are tiny.

It is reported that the HIV remains viable in the lymphoid organs, the main viral reservoir sites, even when sufficient concentration of the anti-HIV drug is available in the blood circulation (Temesgen, Warnke, & Kasten, 2006). The majority of the antiretroviral drugs (including LPV) are unable to reach these viral reservoir sites (Pomerantz, 2002). Hence, for better therapeutic efficacy, it is desirable to have higher amounts of LPV for longer duration of time in lymphoid organs (liver, spleen and lymph nodes) (Wong, Chattopadhyay, Wu, & Bendayan, 2010). Therefore, in conclusion, LPV loaded PANPs could be better alternative than free LPV for treatment of HIV infection and prevention of its relapse.

4. Conclusion

We have shown that hydrophobically modified pullulan nanoparticles are promising carriers to improve oral bioavailability of LPV. The method used in manufacture of PANPs was robust and yielded nearly monodisperse particles of nanometric size (~200 nm) and high entrapment efficiency (~75%). Compared to the free drug, we also demonstrated that LPV in PANPs was metabolized to a lesser extent in the gut. Moreover, metabolic protection and lymphatic uptake of PANPs helped in achieving a significantly higher bioavailability of LPV (~2 folds) than free drug. We have also shown that PANPs distributed to a greater extent to the lymphoid organs, that are also the viral reservoir sites in HIV infection. In summary, LPV loaded PANPs could prove effective in addressing a major delivery challenge for anti-HIV drugs in reaching the viral reservoir sites that are normally inaccessible by conventional therapy. Finally, this investigation can form the basis for the use of hydrophobically modified pullulan in designing lymph-targeted nanoparticles for oral delivery of other HIV-protease inhibitors.

Conflict of interest

The authors declare that they have no conflicts of interest to disclose.

Funding

The authors are grateful to Department of Science and Technology (DST), Science and Engineering Research Council (SERC), New Delhi, India for funding the research under 'Fast Track Scheme for Young Scientists'.

References

Akiyoshi, K., Deguchi, S., Moriguchi, N., Yamaguchi, S., & Sunamoto, J. (1993). Self-aggregates of hydrophobized polysaccharides in water. Formation and characteristics of nanoparticles. *Macromolecules*, *26*, 3062–3068.

Albanese, A., Tang, P. S., & Chan, W. C. (2012). The effect of nanoparticle size, shape, and surface chemistry on biological systems. *Annual Review of Biomedical Engineering*, *14*, 1–16.

Byun, Y., Hwang, J. B., Bang, S. H., Darby, D., Cooksey, K., Dawson, P. L., et al. (2011). Formulation and characterization of α-tocopherol loaded poly-caprolactone (PCL) nanoparticles. *LWT - Food Science and Technology*, *44*, 24–28.

Chandwani1, A., & Shuter, J. (2008). Lopinavir/ritonavir in the treatment of HIV-1 infection: A review. *Therapeutics and Clinical Risk Management*, *4*, 1023–1033.

du Plooy, M., Viljoen, M., & Rheeders, M. (2011). Evidence for time dependent interactions between ritonavir and lopinavir/ritonavir plasma levels following P-glycoprotein inhibition in Sprague-Dawley rats. *Biological and Pharmaceutical Bulletin*, *34*, 66–70.

Farmer, P., Léandre, F., Mukherjee, J., Gupta, R., Tarter, L., & Kim, J. Y. (2001). Community-based treatment of advanced HIV disease: Introducing DOT-HAART (directly observed therapy with highly active antiretroviral therapy). *Bulletin of the World Health Organization*, *79*, 1145–1151.

Feng, S. S. (2004). Nanoparticles of biodegradable polymers for new-concept chemotherapy. *Expert Review of Medical Devices*, *1*, 115–125.

Gajendiran, M., Gopi, V., Elangovan, V., Murali, R. V., & Balasubramanian, S. (2013). Isoniazid loaded core shell nanoparticles derived from PLGA-PEG-PLGA tri-block copolymers: In vitro and in vivo drug release. *Colloids and Surfaces. B, Biointerfaces*, *104*, 107–115.

Haase, A. T. (1999). Population biology of HIV-1 infection: Viral and CD4+ T cell demographics and dynamics in lymphatic tissues. *Annual Review of Immunology*, *17*, 625–656.

Hong, G. Y., Jeong, Y. I., Lee, S. J., Lee, E., Oh, J. S., & Lee, H. C. (2011). Combination of paclitaxel- and retinoic acid-incorporated nanoparticles for the treatment of CT-26 colon carcinoma. *Archives of Pharmacal Research*, *34*, 407–417.

Hunter, A. C., Elsom, J., Wibroe, P. P., & Moghimi, S. M. (2012). Polymeric particulate technologies for oral drug delivery and targeting: A pathophysiological perspective. *Nanomedicine*, *1*, S5–S20.

ICH Q 1 A (R2). Stability testing of new drug substances and products. (CPMP/ICH/2736/99). http://www.emea.eu.int/pdfs/human/ich/273699en.pdf [accessed 25.05.13].

Kaletra® (lopinavir/ritonavir). http://www.rxabbvie.com/pdf/kaletratabpi.pdf [accessed 22.05.13].

Kingsley, J. D., Dou, H., Morehead, J., Rabinow, B., Gendelman, H. E., & Destache, C. J. (2006). Nanotechnology: A focus on nanoparticles as a drug delivery system. *Journal of Neuroimmune Pharmacology*, *1*, 340–350.

Kumari, A., Yadav, S. K., & Yadav, S. C. (2010). Biodegradable polymeric nanoparticles based drug delivery systems. *Colloids and Surfaces. B, Biointerfaces*, *75*, 1–18.

Leathers, T. D. (2003). Biotechnological production and applications of pullulan. *Applied Microbiology and Biotechnology*, *62*, 468–473.

Lee, S. J., Hong, G. Y., Jeong, Y. I., Kang, M. S., Oh, J. S., Song, C. E., et al. (2012). Paclitaxel-incorporated nanoparticles of hydrophobized polysaccharide and their antitumor activity. *International Journal of Pharmaceutics*, *433*, 121–128.

Lee, A., Tsai, H. Y., & Yates, M. Z. (2010). Steric stabilization of thermally responsive N-isopropylacrylamide particles by poly(vinyl alcohol). *Langmuir*, *26*, 18055–18060.

Levy, J. A. (2007). *HIV and the pathogenesis of AIDS* (3rd ed.). Washington, DC: American Society of Microbiology Press.

Li, S. D., & Huang, L. (2008). Pharmacokinetics and biodistribution of nanoparticles. *Molecular Pharmaceutics*, *5*, 496–504.

Mohammad, B. J., Khosro, A., Hadi, V., Mohammad, R. S. S., Ali, N., Yadollah, O., et al. (2008). Kinetic analysis of drug release from nanoparticles. *Journal of Pharmacy & Pharmaceutical Sciences*, *11*, 167–177.

Motozato, Y., Ihara, H., Tomoda, T., & Hirayama, C. (1986). Preparation of gel permeation chromatographic properties of pullulan spheres. *Journal of Chromatography*, *355*, 434.

Pinto, R. C., Neufeld, R. J., Ribeiro, A. J., & Veiga, F. (2006). Nanoencapsulation I. Methods for preparation of drug-loaded polymeric nanoparticles. *Nanomedicine*, *2*, 8–21.

Pomerantz, R. J. (2002). Reservoirs of human immunodeficiency virus type 1: The main obstacles to viral eradication. *Clinical Infectious Disease*, *34*, 91–97.

Ravi, P. R., Aditya, N., Kathuria, H., Malekar, S., & Vats, R. (2013). Lipid nanoparticles for oral delivery of raloxifene: Optimization, stability, in vivo evaluation and uptake mechanism. *European Journal of Pharmaceutics and Biopharmaceutics*, http://dx.doi.org/10.1016/j.ejpb.2013.12.015 [epub ahead of print, accessed 09.02.13]

Ravi, P. R., Vats, R., Dalal, V., Gadekar, N., & Aditya, N. (2013). Design, optimization and evaluation of Poly-ε-Caprolactone (PCL) based polymeric nanoparticles for oral delivery of lopinavir. *Drug Development and Industrial Pharmacy*, http://dx.doi.org/10.3109/03639045.2013.850710 [epub ahead of print, accessed 09.02.13]

Ravi, P. R., Vats, R., Thakur, R., Srivani, S., & Aditya, N. (2012). Effect of grapefruit juice and ritonavir on pharmacokinetics of lopinavir in Wistar rats. *Phytotherapy Research*, *26*, 1490–1495.

Schrager, L. K., & D'Souza, M. P. (1998). Cellular and anatomical reservoirs of HIV-1 in patients receiving potent antiretroviral combination therapy. *The Journal of the American Medical Association*, *280*, 67–71.

Shafran, S. D., Mashinter, L. D., & Roberts, S. E. (2005). The effect of low dose ritonavir monotherapy on fasting serum lipid concentrations. *HIV Medicine*, *6*, 421–425.

Shah, M., & Pathak, K. (2010). Development and statistical optimization of solid lipid nanoparticles of simvastatin by using 2^3 full-factorial design. *AAPS PharmSciTech*, *11*, 489–496.

Sundar, S., Kundu, J., & Kundu, S. C. (2010). Biopolymeric nanoparticles. *Science and Technology of Advanced Materials*, *11*, 014104.

Temesgen, Z., Warnke, D., & Kasten, M. J. (2006). Current status of antiretroviral therapy. *Expert Opinion on Pharmacotherapy*, *7*, 1541–1554.

Trevaskis, N. L., Charman, W. N., & Porter, C. J. (2008). Lipid-based delivery systems and intestinal lymphatic drug transport: A mechanistic update. *Advanced Drug Delivery Reviews*, *60*, 702–716.

Vats, R., Murthy, A. N., & Ravi, P. R. (2011). Simple, rapid and validated LC determination of lopinavir in rat plasma and its application in pharmacokinetic studies. *Scientia Pharmacetica*, *79*, 849–863.

Wong, H. L., Chattopadhyay, N., Wu, X. Y., & Bendayan, R. (2010). Nanotechnology applications for improved delivery of antiretroviral drugs to the brain. *Advanced Drug Delivery Reviews*, *62*, 503–515.

Yao, F., & Weiyuan, J. K. (2010). Drug release kinetics and transport mechanisms of nondegradable and degradable polymeric delivery systems. *Expert Opinion on Drug Delivery*, *7*, 429–444.

Yue, P. F., Lu, X. Y., Zhang, Z. Z., Yuan, H. L., Zhu, W. F., Zheng, Q., et al. (2009). The study on the entrapment efficiency and in vitro release of puerarin submicron emulsion. *AAPS PharmSciTech*, *10*, 376–383.

Zeldin, R. K., & Petruschke, R. A. (2004). Pharmacological and therapeutic properties of ritonavir-boosted protease inhibitor therapy in HIV-infected patients. *Journal of Antimicrobial Chemotherapy*, *53*, 4–5.

Zhang, H. Z., Gao, F. P., Liu, L. R., Li, X. M., Zhou, Z. M., Yang, X. D., et al. (2009). Pullulan acetate nanoparticles prepared by solvent diffusion method for epirubicin chemotherapy. *Colloids and Surfaces. B, Biointerfaces*, *71*, 19–26.